

Version: December 3, 2024

Fractal and Multifractal Analysis of the Rise of Oxygen in Earth's Early Atmosphere

Satish Kumar

Zdzislaw E. Musielak

Manfred Cuntz

Department of Physics, University of Texas at Arlington

Arlington, TX 76019;

`satish.kumar@mavs.uta.edu; zmusielak@uta.edu; cuntz@uta.edu`

ABSTRACT

The rise of oxygen in Earth's atmosphere that occurred 2.4 to 2.2 billion years ago is known as the Earth's Great Oxidation, and its impact on the development of life on Earth was profound. The proposed underlying mathematical models are based on physical parameters whose values are currently not well-established owing to uncertainties in geological and biological data. In this paper, a previously developed model of Earth's atmosphere is modified by adding different strengths of noise to account for the parameters' uncertainties. The effects of the noise on time variations of oxygen, carbon and methane in Earth's early atmosphere are investigated by using fractal and multifractal analysis. We show that these time variations cannot properly be described by a single fractal dimension because they exhibit multifractal characteristics. The obtained results also demonstrate that our time series exhibit the multifractality caused by the long-range time correlations.

Subject headings: Earth's Great Oxidation, Hurst exponent, fractal dimension, multifractal analysis.

1. INTRODUCTION

Fractal methods are well-suited for describing trends in data, specifically, self-similarity, jaggedness and correlation of data sets. Typically, the data is characterized by the so-called fractal dimension, which can be evaluated by finding how the data fills its embedding space (Mandelbrot 1982). The data can be plotted and then the jaggedness of such graph can be compared to a straight line, leading to the box counting method or correlation integral methods. Another way is to treat the data as discrete and to make a comparison to uncorrelated noise, like in the well-known Hurst exponent method (Hurst 1951). The fractal methods are generalized by multifractal methods that require different Hurst exponents at different scales, which means that it is necessary to determine the so-called singularity spectrum (e.g., Falconer 1990; Gouyet 1996).

The fractal and multifractal methods have been extensively applied to different problems in natural sciences, engineering, medicine, and the social sciences (e.g., Falconer 1990; Gouyet 1996; Peitgen et al. 2003; Wu et al. 2007; Lopes & Betrouni 2009). However, to the best of our knowledge, these methods have not yet been directly applied within the recently established field astrobiology or its terrestrial counterparts as, e.g., biogeology. Therefore, in this paper, we first present such applications, which is a topic of great importance, namely, the rise of oxygen in Earth’s early atmosphere, also known as the Earth’s Great Oxidation. Let us begin by describing the problem and then explain our reasons for choosing the fractal and multifractal methods to pursue this study.

The Earth’s Great Oxidation occurred 2.4 to 2.2 billion years ago and it had a significant impact on Earth’s atmospheric physics and chemistry and, furthermore, entailed profound implications for the evolution of life. During the Great Oxidation the atmospheric oxygen concentration rose from less than 10^{-5} of the present atmospheric level (PAL) to more than 0.01 PAL and possibly above 0.1 PAL (e.g., Brocks et al. 1999; Catling et al. 2001; Kasting 2001; Kasting & Siefert 2002). The rise of oxygen itself is a topic of lively discussion owing to its wide ramifications regarding terrestrial and planetary astrobiology; specifically, it is still unclear whether Earth’s Great Oxidation occurred relatively smoothly or exhibited big jumps, i.e., akin to a yoyo model; see Kasting (2006). Moreover, it could also have occurred by exhibiting more intricated mathematical structures, which if present could only be uncovered by multifractal analysis.

Information on the relatively sudden rise of oxygen is in part based on studies of mass-independent fractionation (MIF) of the sulfur isotope ^{33}S (Farquhar et al. 2000). Deviations from $\Delta^{33}\text{S} = 0$ indicate $\text{O}_2 < 10^{-5}$ PAL, so this strong constraint applies to the periods 3.83–3.77 Gyr, 3.50–3.25 Gyr and 2.74–2.45 Gyr ago, noting that the abrupt and permanent end of the strong MIF for times succeeding 2.45 Gyr is very well pronounced. For the time

period from 2.75 to 2.45 Gyr, the behavior of $\Delta^{33}\text{S}$ is closely mirrored by a sudden increase of proxy constraints of palaeo-oxygen, which may potentially be consistent with yoyo-type or fractal behavior, although it fails to offer ultimate support. Evidence that highly fluctuating O_2 levels could have existed already about 3.0 Gyr ago was described by Ohmoto et al. (2006) indicating that the Earth’s oxygen level first increased considerably while decreasing again 0.2 Gyr thereafter.

The increase of O_2 in Earth’s early atmosphere remains a topic of previous and on-going investigations (e.g. Claire et al. 2006; Lyons 2007; Kaufman et al. 2007; Kump 2008; Balk et al. 2009; Frei et al. 2009; Freund et al. 2010; Freund 2011; Flannery & Walter 2012). A set of nonlinear equations describing the time evolution of oxygen, methane and carbon in Earth’s early atmosphere was originally proposed and solved by Goldblatt et al. (2006), thereafter GLW06, who encountered bistability in the system equations, which in their model represent the ancient Earth’s low-oxygen state ($\lesssim 10^{-5}$ PAL) and the high-oxygen state (5×10^{-3} PAL). Subsequent work by Cuntz et al. (2009), thereafter CRM09, on the non-linear set of equations further explored this system by replacing the original step function (GLW09) representing the reductant input rate by more realistic functions (i.e., exponential decay function, logistic decay function) with and without Gaussian white noise. Based on the transition stability analysis for the system equations, a set of non-autonomous, nonlinear differential equations, as well as the inspection of the Lyapunov exponents (e.g., Baker & Gollub 1990; Hilborn 1994; Musielak & Musielak 2009), CRM09 found that the equations do not show chaotic behavior and that the rise of oxygen occurred relatively smoothly.

The models of Earth’s Great Oxidation previously considered were based on a certain set of physical parameters that were determined using the available geological data as summarized by GLW06 and CRM09. However, it is well-known that this set of parameters is not unique because of potentially large uncertainties in the data. Therefore, it is the aim of the present work to expand those previous studies by adopting other sets of parameters and also analyzing the obtained results by using fractal and multifractal techniques. Specifically, we will use the standard Hurst exponent (Hurst 1951) and the fractal dimension related to it (Mandelbrot 1982), as well as the Multifractal Detrended Fluctuation Analysis (MFDFA) (Kantelhardt et al. 2002), which was originally developed for non-stationary time series and required the so-called generalized Hurst exponents for computing a width of singularity spectrum (WSS). Our choice of using the MFDFA is motivated by the fact that our numerical solutions constitute non-stationary time series.

Our studies are performed for different strengths of white Gaussian noise, which is added to the system to account for possible variations in the physical parameters as well as for uncertainties in the adopted values of the parameters. We consider different levels

of noise in the system and investigate their effects on the rise of oxygen as well as on the associated time variations of carbon and methane in the early Earth’s atmosphere. These effects of the noise are investigated by performing fractal and multifractal analyses of our numerical results. We perform the analyses to demonstrate that no single fractal dimension can be used to describe time variations of oxygen, carbon and methane because they exhibit multifractal characteristics due to long-range correlations of the small and large fluctuations in the time series.

Our paper is structured as follows: In §2, we describe the system equations considered in our study, the numerical method of solution, and the methods for performing the fractal and multifractal analysis. In §3, we present our results and discussion. Our conclusions are given in §4.

2. FORMULATION AND ANALYSIS TECHNIQUES

2.1. Original Governing Equations

The set of equations was originally given by GLW06 and was subsequently revisited by CRM09. It encompasses a simplified model of Earth’s global redox system, representing the atmosphere, ocean, and crust. Concerning the atmosphere and ocean, the number of moles of methane \mathcal{M} (CH_4) and oxygen \mathcal{O} (O_2) are calculated. Furthermore, with respect to the ocean floor, the amount of buried organic carbon \mathcal{C} in the crust is also computed. This leads to the following system of equations:

$$\frac{d\mathcal{M}}{dt} = \frac{1}{2}\Omega_{(\text{O}_2)}(N + r) - \frac{1}{2}\Psi_{(\text{O}_2)}\mathcal{M}^{0.7} - s\mathcal{M} - \frac{1}{2}\Omega_{(\text{O}_2)}[\beta(N + r) - w\mathcal{C}] , \quad (1)$$

$$\frac{d\mathcal{O}}{dt} = \Omega_{(\text{O}_2)}N - (1 - \Omega_{(\text{O}_2)})r - \Psi_{(\text{O}_2)}\mathcal{M}^{0.7} - s\mathcal{M} - (1 - \Omega_{(\text{O}_2)})[\beta(N + r) - w\mathcal{C}] , \quad (2)$$

and

$$\frac{d\mathcal{C}}{dt} = \beta(N + r) - w\mathcal{C} . \quad (3)$$

This set of differential equations is coupled and nonlinear because of the term $\mathcal{M}^{0.7}$ as well as the functions $\Omega_{(\text{O}_2)}$ and $\Psi_{(\text{O}_2)}$. Note that $\Omega_{(\text{O}_2)}$ is given as $\Omega_{(\text{O}_2)} = (1 - \gamma)(1 - \delta)$ with $\gamma = \mathcal{O}/(d_\gamma + \mathcal{O})$ and $\delta = \mathcal{O}/(d_\delta + \mathcal{O})$, whereas $\Psi_{(\text{O}_2)}$ is given as $\Psi_{(\text{O}_2)} = 10^\epsilon$ with $\epsilon = a_1\varphi^4 + a_2\varphi^3 + a_3\varphi^2 + a_4\varphi + a_5$, $\varphi = \log \mathcal{O}$, $a_1 = 0.0030$, $a_2 = -0.1655$, $a_3 = 3.2305$, $a_4 = -25.8343$ and $a_5 = 71.5398$.

The different terms, parameters, and variables of Eqs. (1) to (3) require further detailed explanations. The first term on the RHS of $d\mathcal{M}/dt$ and the corresponding terms of $d\mathcal{O}/dt$ denote the net primary productivity for oxygenic photosynthesis N and the net input of reductant to the surface r , an electron donor for anoxygenic photosynthesis, which both depend on the time-variable oxygen concentration \mathcal{O} . Both GLW06 and CRM09 took $N = 3.75 \times 10^{15} \text{ mol O}_2 \text{ yr}^{-1}$. However, for $r = r(t)$, for which GLW06 chose a step function, exhibiting a downward jump from 3×10^{11} to $7.5 \times 10^{10} \text{ mol O}_2 \text{ equiv. yr}^{-1}$ at 2.4 Gyr, CRM09 adopted different functions, including functions incorporating statistical noise. This allowed them to consider the impact of different plausible reductant functions on early Earth’s atmospheric chemistry.

The work by GLW06 and CRM09 considered the dominant processes of the marine biosphere related to oxygenic photosynthesis and represented by an assumed net primary productivity of $N \text{ mol O}_2 \text{ yr}^{-1}$, implying that the total organic carbon produced is given as $(N + r)$. The fraction of this amount consumed by heterotrophic respirers is $\gamma = \mathcal{O}/(d_\gamma + \mathcal{O})$ with $d_\gamma = 1.36 \times 10^{19} \text{ mol}$. The fraction of the methane produced that is consumed by methanotrops is given as $\delta = \mathcal{O}/(d_\delta + \mathcal{O})$, where $d_\delta = 2.73 \times 10^{17} \text{ mol}$. Therefore, the fraction of the oxygen and methane produced that reaches the atmosphere is given by $\Omega_{(\text{O}_2)} = (1 - \gamma)(1 - \delta)$. The next two terms on the RHS of Eqs. (1) and (2) correspond to the atmospheric methane oxidation reaction. Its rate can be obtained by fitting the results of detailed photochemical models, including the introduction of $\Psi_{(\text{O}_2)}$, which constitutes a polynomial function with respect to the amount of oxygen. Once there is sufficient oxygen, Earth’s ozone layer forms, thus providing an effective shield against UV radiation. There are other terms in Eqs. (1) and (2) related to sinks and sources of atmospheric methane \mathcal{M} . Methane can be nullified by oxidation, but it can be lost through hydrogen escape since methane is considered to be the sole source of hydrogen in the upper atmosphere with $s = 3.7 \times 10^{-5} \text{ yr}^{-1}$ (Goldblatt 2008) as a limiting flux constant. The final terms on the RHS of Eqs. (1) to (3) are due to the amount of buried organic carbon, which depends on the fraction β , taken as 2×10^{-3} , of the total organic carbon $(N + r)$ that is produced. The rate of organic carbon weathering is $w\mathcal{C}$, where the bulk weathering rate w , given as $w = 6 \times 10^{-9} \text{ yr}^{-1}$, is set by analogy to present conditions and \mathcal{C} is the crustal organic carbon; see GLW06 and CRM09 for further details.

GLW06 obtained steady state solutions for methane and carbon given as $\mathcal{M} = r/s$ and $\mathcal{C} = \beta(N + r)/w$, respectively. In case of oxygen the steady state solution required obtaining the roots of a more complicated equation. In GLW06’s model, the solutions for oxygen, methane and carbon, exhibit bistability. This result, as previously pointed out by Kasting (2006), arguably offers crucial insights into the bistable nature of Earth’s atmosphere, especially pertaining to the Great Oxidation, considering that the latter constitutes a switch to

the high-oxygen (more than 5×10^{-3} PAL) steady state from a previous low-oxygen (less than 10^{-5} PAL) steady state that existed for at least 300 million years even after the onset of oxygenic photosynthesis.

2.2. Modified Governing Equations with Noise

The main objective of our work is to add white Gaussian noise to the governing equations, i.e., Eqs. (1) to (3), in order to investigate its effect on the rise of oxygen in the early Earth’s atmosphere. We therefore introduce the following three new variables: $\eta_{\mathcal{M}} = \sigma\kappa\mathcal{M}$, $\eta_{\mathcal{O}} = \sigma\kappa\mathcal{O}$, and $\eta_{\mathcal{C}} = \sigma\kappa\mathcal{C}$, where σ is the strength of noise ranging from 0.005 to 0.010, and κ is a random number given by a normal distribution with a mean of 0 and a variance of 1. Furthermore, \mathcal{M} , \mathcal{C} , and \mathcal{O} represent the amounts of methane, carbon, and oxygen, respectively, as before. With the new variables added, Eqs. (1) to (3) read as

$$\frac{d\mathcal{M}}{dt} = \frac{1}{2}\Omega_{(\text{O}_2)}(N + r) - \frac{1}{2}\Psi_{(\text{O}_2)}\mathcal{M}^{0.7} - s\mathcal{M} - \frac{1}{2}\Omega_{(\text{O}_2)}[\beta(N + r) - w\mathcal{C}] + \eta_{\mathcal{M}}, \quad (4)$$

$$\frac{d\mathcal{O}}{dt} = \Omega_{(\text{O}_2)}N - (1 - \Omega_{(\text{O}_2)})r - \Psi_{(\text{O}_2)}\mathcal{M}^{0.7} - s\mathcal{M} - (1 - \Omega_{(\text{O}_2)})[\beta(N + r) - w\mathcal{C}] + \eta_{\mathcal{O}}, \quad (5)$$

and

$$\frac{d\mathcal{C}}{dt} = \beta(N + r) - w\mathcal{C} + \eta_{\mathcal{C}}. \quad (6)$$

These equations are solved using the geological and Earth’s atmospheric data as discussed by GLW06 and CRM09 (see §2.1). However, the new variables $\eta_{\mathcal{M}}$, $\eta_{\mathcal{O}}$, and $\eta_{\mathcal{C}}$ allow us to consider appropriate levels of noise for the terms $d\mathcal{M}/dt$, $d\mathcal{O}/dt$, and $d\mathcal{C}/dt$, respectively, in the view of inherent uncertainties in the underlying geological processes.

Equations (4) to (6) are solved for different values of the noise strength σ by using the Euler-Maruyama method, which is suitable for the considered set of equations; additionally, the resulting numerical errors are small. The obtained numerical results are displayed in 3D phase space defined by the variables \mathcal{O} , \mathcal{C} and \mathcal{M} . We refer to such displays of our results as phase portraits whose main advantage is that they are able to show relationships between the three variables, and, furthermore, allow to demonstrate how the relationships change when the noise strength σ is varied. In order to determine how effectively the change occurs, we use the standard Hurst exponent (Hurst 1951) and fractal dimension related to this exponent (Mandelbrot 1982) as well as the so-called multifractal technique, which we now describe in detail.

2.3. Analysis Techniques

2.3.1. Hurst Exponent and Fractal Dimension

The standard Hurst exponent h was originally introduced by Hurst (1951), who demonstrated that data described by h is anti-correlated if $0 \leq h < 0.5$, uncorrelated if $h = 0.5$, and correlated if $0.5 < h \leq 1.0$. According to Mandelbrot (1982), h can be used to introduce the fractal dimension $D_h = \epsilon - h$, where ϵ is the embedding space, and D_h is given as

$$\begin{aligned} D_h &= \frac{1}{1-h} \quad 0 \leq h < 0.5 \quad (\text{anti-persistent}) \\ D_h &= 2.0 \quad h = 0.5 \quad (\text{non-persistent}) \\ D_h &= \frac{1}{h} \quad 0.5 < h \leq 1.0 \quad (\text{persistent}) . \end{aligned} \quad (7)$$

The above definition of D_h is known to provide a smooth transition from anti-persistent to persistent including the point $h = 0.5$, and to be robust for measuring macro-trends in the data Gouyet (1996).

2.3.2. Multifractal Technique

We also analyze the results of our numerical simulations by using the Multifractal Detrended Fluctuation Analysis (MFDFA), which is used to compute the so-called generalized Hurst exponents $h(q)$ and a width of singularity spectrum; note that the generalized Hurst exponents $h(q)$ becomes the standard Hurst exponent h if $q = 2$. Let us now briefly describe the MFDFA method by following the notation and steps originally introduced by Kantelhardt et al. (2002). We begin with calculating the profile for a given series $Y(i)$, where $i = 1, 2, \dots, N$, using

$$Y(i) = \sum_{k=1}^i [x_k - \langle x \rangle] , \quad (8)$$

profile into $N_s = N/s$ non-overlapping segments of equal length s . In general, N may not be a multiple of s , thus in order to account for a small part remaining at the end of the series, we repeat the same procedure but this time by starting from the end of the series; note that reverting the series does not affect the multifractal behavior of the series as all its parameters remain the same. Since the procedure is used twice, we obtain $2N_s$ segments.

We determine a possible local trend of the series by the least-square polynomial fit of the series. Thereafter, we calculate the variance by using

$$F^2(\nu, s) = \frac{1}{s} \sum_{i=1}^s [Y((\nu - 1)s + i) - y_\nu(i)]^2 , \quad (9)$$

for the segments $\nu = 1, 2, \dots, N_s$, and

$$F^2(\nu, s) = \frac{1}{s} \sum_{i=1}^s [Y(N - (\nu - N_s)s + i) - y_\nu(i)]^2 , \quad (10)$$

for the segments $\nu = N_s + 1, \dots, 2N_s$, with $y_\nu(i)$ being the fitting polynomial in segment ν .

With the variance known, we compute the moment dependent fluctuation function

$$F_q(s) = \left[\frac{1}{2N_s} \sum_{\nu=1}^{2N_s} [F^2(\nu, s)]^{q/2} \right]^{1/q} . \quad (11)$$

Note that for $q = 2$, the above analysis becomes the detrended fluctuation analysis (DFA). However, for other values of q , the multifractal behavior is characterized by different Hurst exponents at different scales, the so-called generalized Hurst exponent, which requires the computation of the fluctuating function at different moments.

The power law behavior is displayed in log-log plots of the fluctuating function $F_q(s) \approx s^{h(q)}$, where the generalized Hurst exponent $h(q)$ converges to the standard Hurst exponent h of the series. Since scales $s < 10$ and $s > N/4$ lead to systematic statistical errors, we take the values between them. Moreover, $F_q(s)$ diverges for $q = 0$, which means that it cannot be calculated using Eq. (9); therefore, we compute it by using a logarithmic average given as

$$F_q(s) = \exp \left[\frac{1}{4N_s} \sum_{\nu=1}^{2N_s} \ln [F^2(\nu, s)] \right] - s^{h(0)} . \quad (12)$$

The generalized Hurst exponent is related to the classical scaling exponent $\tau(q)$ through the following relation $\tau(q) = qh(q) - 1$.

There is also another way of characterizing the multifractal series. It involves introducing the so-called singularity spectrum $f(\xi)$, which is related to $\tau(q)$ via a Legendre transform, i.e., $\xi = \tau'(q)$ and $f(\xi) = q\xi - \tau(q)$, with ξ being the singularity strength or Hölder exponent; note that the WSS provides a measure of strength of multifractal behavior, and that it is used in this study to analyze the results of our numerical simulations.

3. RESULTS AND DISCUSSION

3.1. Numerical Results

We solve Eqs. (4) through (6) by using the Euler-Maruyama method. The input parameter $r(t)$, i.e., the net input of reductant to the surface, is specified as given by the exponential function $r(t) = r_0 \exp(-\alpha t/t_0)$, with $r_0 = 3.5 \times 10^{11}$ mol O₂ equiv. yr⁻¹, $\alpha = 1.4$, and $t_0 = 1.0 \times 10^7$ yr. In addition, we assume that the initial number of oxygen molecules is 10^8 mol and use a stepsize of 10^{-3} yr. Our numerical computations indicate time-dependent changes for the amounts of oxygen, methane and carbon. The changes of oxygen in time are presented in Fig. 1, which shows an initially smooth, but steep rise within the first 10^3 years, and then oscillatory behavior, which is driven by the noise. It is this oscillatory behavior that we want to investigate further in the 3D phase space defined by the variables describing carbon, oxygen and methane of the system.

The obtained phase portraits for different strengths of noise are shown in Fig. 2, although our numerical results obtained for the first 10^3 years have been omitted. The phase portraits show the relationships between the carbon, oxygen and methane variables and the extend of 3D phase space covered by these relationships for the different levels of noise. By inspecting the phase portraits of Fig. 2, we find that a different strength of noise corresponds to a remarkably different picture attained in the phase space. However, there is not a clear correlation between the strength of noise and the volume of the 3D phase space covered by the relationships. Therefore, as the next step we perform the fractal and multifractal analysis of our numerical results.

Though this analysis, we want to determine whether the resulting numerical time series describing variations of carbon, oxygen and methane in our model of Earth's early atmosphere is a fractal system that requires a single exponent or fractal dimension, or a multifractal system that is characterized by a continuous spectrum of exponents or the WSS. The analysis will also allow us to identify the nature of multifractality, i.e., whether it is due to probability distributions or long-range correlations.

3.2. Generalized Hurst exponent and fractal dimension

We computed the generalized Hurst exponent h by using the MFDFA and taking $q = 2$, which means that the resulting h is equivalent to the standard Hurst exponent (Hurst 1951). The values of h obtained for different strengths of the noise introduced to the system are shown in the second column of Table 1. It is seen that h is not sensitive to different values of

the noise strengths and that it is close to 0.5, which implies that the numerically computed time series data is uncorrelated.

Having obtained h , we used the results presented in §2.3 to calculate the fractal dimension D_h . The computed values of D_h are given in the third column of Table 1. It is seen that D_h is largely independent of the strength of the noise, which is an expected result because of the D_h dependence on h . This obviously implies that our numerically computed time series of variations of carbon, oxygen and methane in our model of Earth’s early atmosphere cannot be fully characterized by one single exponent or fractal dimension. Therefore, our main conclusions about the effects of noise on our numerical results must arise from the multifractal analysis and its concept of the WSS.

3.3. Multifractal analysis

As already described in §2.3, we performed a multifractal analysis with the MFDFA, which was used to compute the WSS, where the WSS represents the distance between two end points of the singularity spectrum, i.e., the first and last values of the Hölder exponent ξ . The higher the value of the WSS, the stronger the multifractal characteristics of the time series. The computed values of the WSS are given in the last column of Table 1.

It is seen that the value of the WSS is clearly the highest for the strength of noise $\sigma = 0.005$ and the lowest for $\sigma = 0.010$. There is an obvious trend indicating a negative slope between these values in terms of a σ –WSS relationship, albeit the existence of scatter, which is most evident regarding $\sigma = 0.008$, where the value for the WSS is close to the minimum value at $\sigma = 0.010$. In order to gauge the significance of the decline of the WSS values as function of σ , we applied a two-tailed Spearman r correlation analysis (e.g. Press et al. 1986). The Spearman r is identified as -0.71 with a standard deviation of 0.11, hence clearly confirming the suspected functional decline. Thus, the general trend of the decreasing WSS with increasing values of σ appears to be valid for our numerically generated time series. The observed trend is an indication that white Gaussian noise changes the multifractal characteristics of our time series, which is contrary to the fractal dimension that is about the same for all our time series as shown in the third column of Table 1. Therefore, the inclusion of the noise makes a significant contribution to the overall behavior of oxygen, carbon and methane in our model of Earth’s early atmosphere, and our results clearly show that this contribution can only be determined by using the multifractal analysis.

Having established the multifractal characteristics of the time series, we then randomized the series and used the WSS to identify the nature of multifractality. In general, the

multifractality can be either due to a broad probability density function for the values of the time series, or due to different long-range time correlations of the small and large fluctuations in the time series, or both. The obtained results show that our time series exhibit the multifractality caused by the long-range time correlations of the small and large fluctuations in the time series.

This is an important result, as it shows that the numerically generated time series of oxygen, carbon and methane still have some statistical correlations even if they are separated by very long time intervals.

4. CONCLUSIONS

In this study we expand on previous work aimed at modeling the rise of oxygen in Earth’s atmosphere that occurred 2.4 to 2.2 billion years ago and is known as the Earth’s Great Oxidation. Experimentally, information on this process has been obtained through extended biogeological studies; this field of research is obviously of significant importance for historical terrestrial studies, but it has also profound implications for the growing fields of exobiology and planetary science.

In a previous paper, GLW06 presented a mathematical model for the time-dependent behavior of carbon, methane and oxygen based on a set of nonlinear differential equations. This model incorporated numerous geological, atmospheric, biological and biochemical processes, and was able to reproduce the bifurcated nature of Earth’s ancient atmosphere consisting of a low-oxygen (less than 10^{-5} PAL) and a high-oxygen state (more than 5×10^{-3} PAL), including the transition between the two. This model was subsequently extended by CRM09 who studied details of the switch between the two stages using more general step functions for the underlying biogeological process. The aim of this work was to explore whether or not the switch occurred in jumps (yo-yo-model) or exhibited a more gradual oxygen concentration increase.

In the present work we further augmented this model by investigating the effects of the noise on the time variations of oxygen, carbon and methane by using fractal and multifractal analysis techniques. The overall goal was to offer a more realistic picture by accounting for uncertainties in the geological data, which led us to add different strengths of noise within the original equations describing Earth’s ancient atmosphere.

The obtained results show that the numerically generated time series describing the time variations of oxygen, carbon and methane during the time-span of Earth’s Great Oxidation cannot properly be described by a single fractal dimension because they exhibit multifractal

characteristics. We also demonstrated that our time series exhibit the multifractality caused by the long-range time correlations of the small and large fluctuations in the time series. We consider this work as a further step toward elucidating the complex biogeochemical processes of early Earth, which gave rise to the previously identified oxygen increase, among other dynamic developments.

This work has been supported in part by the Alexander von Humboldt Foundation (Z. E. M.), by the University of Texas at Arlington through its Faculty Development Program (Z. E. M.), and by the SETI Institute (M. C.).

REFERENCES

Baker, G. L., & Gollub, J. P. 1990, Chaotic Dynamics: An Introduction, Cambridge, Cambridge University Press

Balk, M., Bose, M., Ertem, G., Rogoff, D. A., Rothschild, L. J., & Freund, F. T. 2009, Earth Pla. Sci. Lett., 283, 87

Brocks, J. J., et al. 1999, Science, 285, 1033

Catling, D. C., Zahnle, K. J., & McKay, C. P. 2001, Science, 293, 839

Claire, M. W., Catling, D. C., & Zahnle, K. J. 2006, Geobiology, 4, 239

Cuntz, M., Roy, D., & Musielak, Z. E. 2009, ApJ, 706, L178 [CRM09]

Falconer, K. 1990, Fractal Geometry. Mathematical Foundations and Applications, New York, John Wiley & Sons

Farquhar, J., Bao, H., & Thiemens, M. 2000, Science, 289, 757

Flannery, D. T., & Walter, M. R. 2012, Australian J. Earth Sciences, 59, 1

Frei, R., Gaucher, C., Poulton S. W., & Canfield, D. E. 2009, Nature, 461, 250

Freund, F. T., Balk, M., & Rothschild, L. J. 2010, Astrobiology Science Conference 2010: Evolution and Life: Surviving Catastrophes and Extremes on Earth and Beyond, League City, Texas, LPI Contribution No. 1538, p. 5640

Freund, F. T. 2011, J. Asian Earth Sciences, 41, 383

Goldblatt, C. 2008, Ph.D. thesis, University of East Anglia

Goldblatt, C., Lenton, T. M., & Watson, A. J. 2006, Nature, 443, 683 [GLW06]

Gouyet, J.-F. 1996, Physics and Fractal Structures, New York, Springer

Hilborn, R. C. 1994, Chaos and Nonlinear Dynamics, Oxford, Oxford University Press

Hurst, H. E. 1951, Trans. Amer. Soc. Civ. Eng., 116, 770

Kantelhardta, J. W., Zschiegnera, S. A., Koscielny-Bunde, E., Havlind, S., Bunde, A., & Stanley, H. E. 2002, Physica A, 316, 87

Kasting, J. F. 2001, Science, 293, 819

Kasting, J. F., & Siefert, J. L. 2002, *Science*, 296, 1066

Kasting, J. F. 2006, *Nature*, 443, 643

Kaufman, A. J., et al. 2007, *Science*, 317, 1900

Kump, L. R. 2008, *Nature*, 451, 277

Lopes, R., & Betrouni, N. 2009, *Medical Image Analysis*, 13, 634

Lyons, T. W. 2007, *Nature*, 448, 1005

Mandelbrot, B. B. 1982, *The Fractal Geometry of Nature*, San Francisco, W. H. Freeman

Musielak, Z. E., & Musielak, D. E. 2009, *Int. J. Bifurcation and Chaos*, 19, 2823

Ohmoto, H., et al. 2006, *Nature*, 442, 908

Peitgen, H.-O., Jürgens, H., & Saupe, D. 2003, *Chaos and Fractals*, 2nd Ed., Berlin, Springer

Press, W. H., Flannery, B. P., Teukolsky, S. A., & Vetterling, W. T. 1986, *Numerical Recipes*, Cambridge (UK), Cambridge University Press

Wu, X., Wang, J., Lu, J., & Iu, H. H. C. 2007, *Chaos, Solitons and Fractals*, 32, 1483

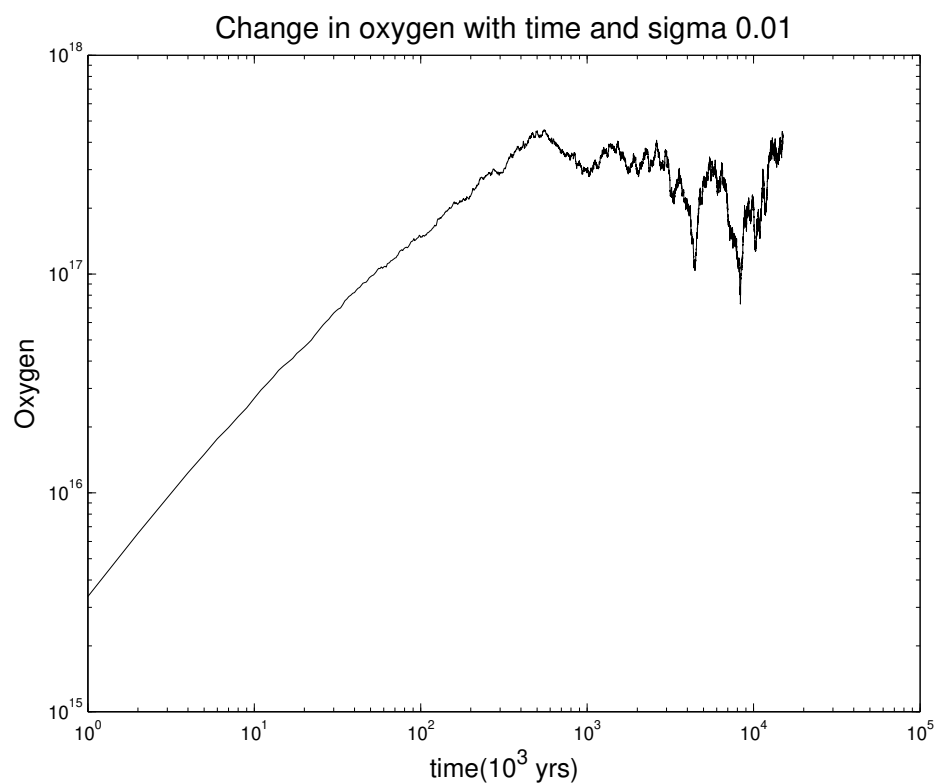


Fig. 1.— Variations of oxygen with time in the early Earth's atmosphere for the strength of noise $\sigma = 0.01$.

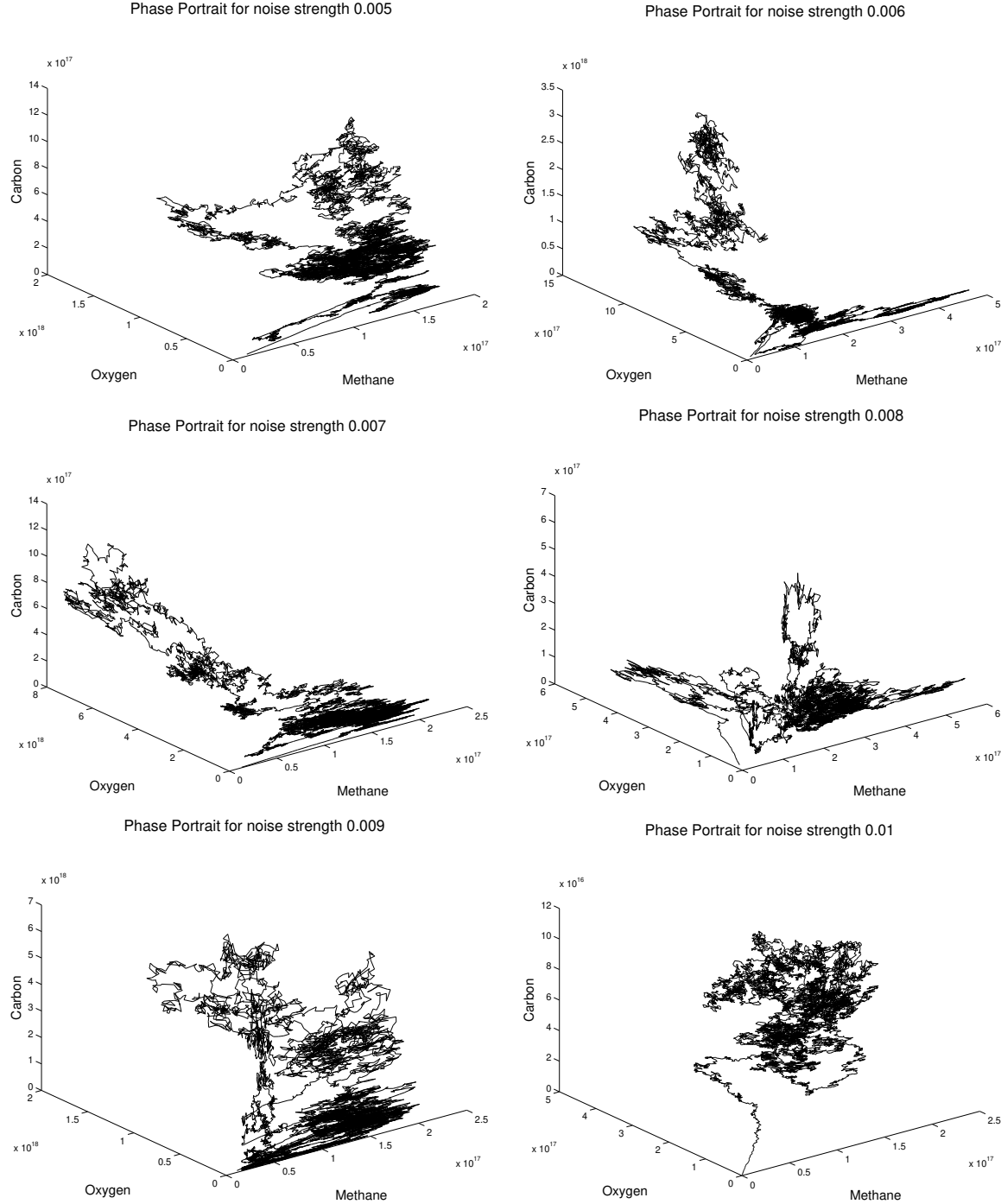


Fig. 2.— Phase portraits of our numerical results obtained for different values of the strength of noise σ in each panel.

Table 1. Fractal and multifractal analysis of numerical results

Noise strength σ	Generalized Hurst exponent h at $q = 2$	Fractal dimension D_h	WSS
0.005	0.5087	2.4913	1.2080
0.006	0.5104	2.4896	1.0760
0.007	0.5032	2.4968	1.1609
0.008	0.5457	2.4543	0.8647
0.009	0.5325	2.4675	1.0918
0.010	0.5206	2.4794	0.8110